

Panaxanthone Isolated from Pericarp of *Garcinia mangostana* L. Suppresses Tumor Growth and Metastasis of a Mouse Model of Mammary Cancer

HITOSHI DOI^{1,2}, MASA-AKI SHIBATA^{1,3}, EIKO SHIBATA³, JUNJI MORIMOTO⁴, YUKIHIRO AKAO⁵, MUNEKAZU IINUMA⁶, NOBUHIKO TANIGAWA² and YOSHINORI OTSUKI^{1,3}

¹Department of Anatomy and Cell Biology, ²Department of General and Gastroenterological Surgery, ³High-Tech Research Center and ⁴Laboratory Animal Center, Osaka Medical College, Osaka 569-8686; ⁵United Graduate School of Drug Discovery and Medical Information Science, Gifu University, Gifu 501-1193; ⁶Gifu Pharmaceutical University, Gifu 502-8585, Japan

Abstract. *Background:* The antitumor growth and antimetastatic activity of panaxanthone (approximately 80% α -mangostin and 20% γ -mangostin) were studied in a mouse metastatic mammary cancer model that produces a metastatic spectrum similar to that seen in human breast cancer. *Materials and Methods:* Mammary tumors, induced by inoculation of syngeneic BALB/c mice with BJMC3879 cells, were subsequently treated with panaxanthone at 0, 2,500, or 5,000 ppm in their diet. *In vitro* studies were also conducted to evaluate the effects of α -mangostin, the main component of panaxanthone, on BJMC3879 cells. *Results:* In the *in vivo* study, tumor volumes were significantly suppressed in mice treated with 2,500 and 5,000 ppm panaxanthone in their diet. The multiplicity of lung metastasis was significantly lower in the 5,000 ppm group. Lymph node metastasis also tended to decrease in the 5,000 ppm group but not significantly. The antitumor effects of panaxanthone were associated with elevation of apoptotic cell death, antiproliferation (inhibition of PCNA) and antiangiogenesis (inhibition of microvessel density). The *in vitro* study demonstrated that α -mangostin induced apoptosis, as evidenced by increased numbers of

TUNEL-positive cells, elevated activities of caspases and a decrease in mitochondrial membrane potential, cell cycle arrest in the G₁-phase and decreases in the cell population in the S- and G₂/M-phases. *Conclusion:* These results suggest that the observed antimetastatic activity of panaxanthone may be of clinical significance as adjuvant therapy in metastatic human breast cancer, and may also be useful as a chemopreventative of breast cancer development.

Recently, many tropical plants have been shown to have interesting biological activities with potential therapeutic applications (1). The fruit hull of the mangosteen (*Garcinia mangostana* L.), which is a tree found in Southeast Asia, has been used as a traditional medicine for the treatment of skin infection, wounds and diarrhea for many years (2). The fruit hull contains various xanthone derivatives including α -mangostin and γ -mangostin. Three xanthones, α -mangostin, β -mangostin and γ -mangostin, are found in the pericarp. Recent studies have revealed that these xanthones exhibit a variety of biological activities including antibacterial (3), anti-inflammatory (4) and anticancer (5-9) effects. Among these compounds, α -mangostin and γ -mangostin have the most potent effects on cancer cells.

Breast cancer is the most common malignancy among women in the Western hemisphere. Whereas a series of consensus statements have established neoadjuvant and adjuvant treatment as well as surgery as state-of-the-art treatment in patients with early breast cancer, only marginal understanding has been reached concerning an internationally accepted consensus on the therapy of metastatic or advanced breast cancer (10). In Japan, 35,000 women develop breast cancer annually and there are 10,000 deaths from the disease (11). In recent years, improvements in chemotherapy and radiotherapy have prolonged life, however, the recovery from recurrent breast cancer is very

Abbreviations: DMSO, Dimethyl sulfoxide; H&E, hematoxylin and eosin; LSC, laser scanning cytometer; $\Delta\Psi$, membrane potential; MMTV, mouse mammary tumor virus; PBS, phosphate-buffered saline; TUNEL, terminal deoxynucleotidyl transferase-mediated dUTP-FITC nick end-labeling; vWF, von Willebrand factor.

Correspondence to: Professor Yoshinori Otsuki, Department of Anatomy and Cell Biology, Division of Life Sciences, Osaka Medical College, 2-7, Daigaku-machi, Takatsuki, Osaka 569-8686, Japan. e-mail: an1000@art.osaka-med.ac.jp

Key Words: α -Mangostin, panaxanthone, antitumor, chemoprevention, mammary cancer.

poor, and the percentage of patients who go into remission and who eventually heal is also low (12).

The development of a new therapeutic approach to breast cancer remains one of the most challenging areas in cancer research. Panaxanthone isolated from pericarp of mangosteen contains 75-85% α -mangostin and 5-15% γ -mangostin. In the present study, we investigated panaxanthone suppression of tumor growth and metastasis *in vivo* in a mouse mammary cancer model. In addition, data produced from our *in vitro* studies of α -mangostin (the main component of panaxanthone) allowed us to identify at least part of the suppression mechanism.

Materials and Methods

Reagents. Panaxanthone (75-85% α -mangostin and 5-15% γ -mangostin) and its main component α -mangostin were obtained from Gifu Pharmaceutical University, Gifu, Japan.

Cells and animals. We established the BJMC3879 mammary adenocarcinoma cell line which shows a high metastatic propensity to lungs and lymph nodes (13), a trait retained through culture. BJMC3879 cells are known to feature a *p53* mutation (14) and were here maintained in Dulbecco's modified Eagle's medium or RPMI-1640 containing 10% fetal bovine serum with streptomycin/penicillin in an incubator under 5% CO₂.

Animal experiment. A total of 42 female 5-week-old BALB/c mice were used in this study (Japan SLC, Hamamatsu, Japan). The animals were housed at 6 per plastic cage in the tumor growth phase on wood chip bedding with free access to water and food under conditions of controlled temperature (21±2°C), humidity (50±10%) and lighting (12/12-h light-dark cycle). Panaxanthone was ground and mixed with a commercial powdered diet (Oriental MF; Oriental Yeast Co., Tokyo, Japan) at appropriate concentrations. All animals were held for a 2-week acclimatization period before study commencement. All manipulations of mice were performed in accordance with the procedures outlined in the Guide for the Care and Use of Laboratory Animals of Osaka Medical College.

Tumor growth study. Based on the results of a separate study (data not shown), the dietary dosages of panaxanthone were chosen as 5,000 ppm for the high-dose diet and 2,500 ppm for the intermediate-dose diet. BJMC3879 cells (5×10⁶ cells/0.3 ml phosphate-buffered saline (PBS)) were inoculated *s.c.* into the right inguinal region of the 42 female BALB/c mice. Two weeks later, when tumors had grown to ~0.8 cm in diameter, groups of 14 mice were administered 0, 2,500, or 5,000 ppm of panaxanthone in their diet for 8 weeks. Individual body weights were recorded weekly. Using calipers, each mammary tumor was also measured weekly and tumor volumes calculated using the following formula: maximum diameter × (minimum diameter)² × 0.4 (15). All animals were killed under anesthesia by exsanguination.

Histopathological analysis. At necropsy, tumors and lymph nodes, routinely those from the axillary and femoral regions and in addition those appearing abnormal, were removed, fixed in 10% formaldehyde solution in phosphate buffer and routinely processed

Table I. Average food consumption and panaxanthone intake.

Panaxanthone (ppm in diet)	Average food consumption (mg/day/mouse)	Average panaxanthone (mg/kg/day/mouse)
0	338	0
2,500	292	543
5,000	290	1078

Groups of 14 mice were given 0, 2500 ppm, or 5000 ppm panaxanthone in their food for 8 weeks. The panaxanthone concentration was calculated based on food consumption and body weight data.

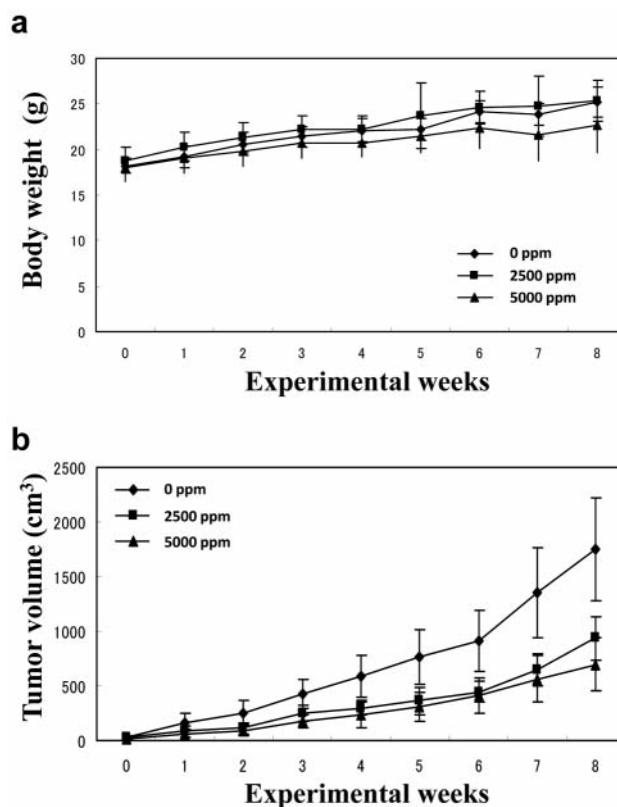


Figure 1. Body weights (a) and tumor volumes (b) in mammary carcinomas from female BALB/c controls and mice treated with 2,500 or 5,000 ppm panaxanthone. Control, 2,500 and 5,000 ppm treated groups consisted of 14 mice each. Data represent mean±SD. (a) There were no significant differences in body weights among the panaxanthone-treated groups and the control group. (b) Tumor growth, as assessed by computed volume, was significantly inhibited in mice receiving panaxanthone at 2,500 and 5,000 ppm from 3 and 2 weeks respectively compared with the control group (*p*<0.01). Data represent mean±SD.

through to paraffin embedding. Lungs were inflated with formaldehyde solution prior to excision and immersion in fixative. The individual lobes were subsequently removed from the bronchial tree, trimmed into seven pieces and examined for metastatic foci before being similarly processed to paraffin embedding. All paraffin-embedded tissues were cut into 4 μm sections, with

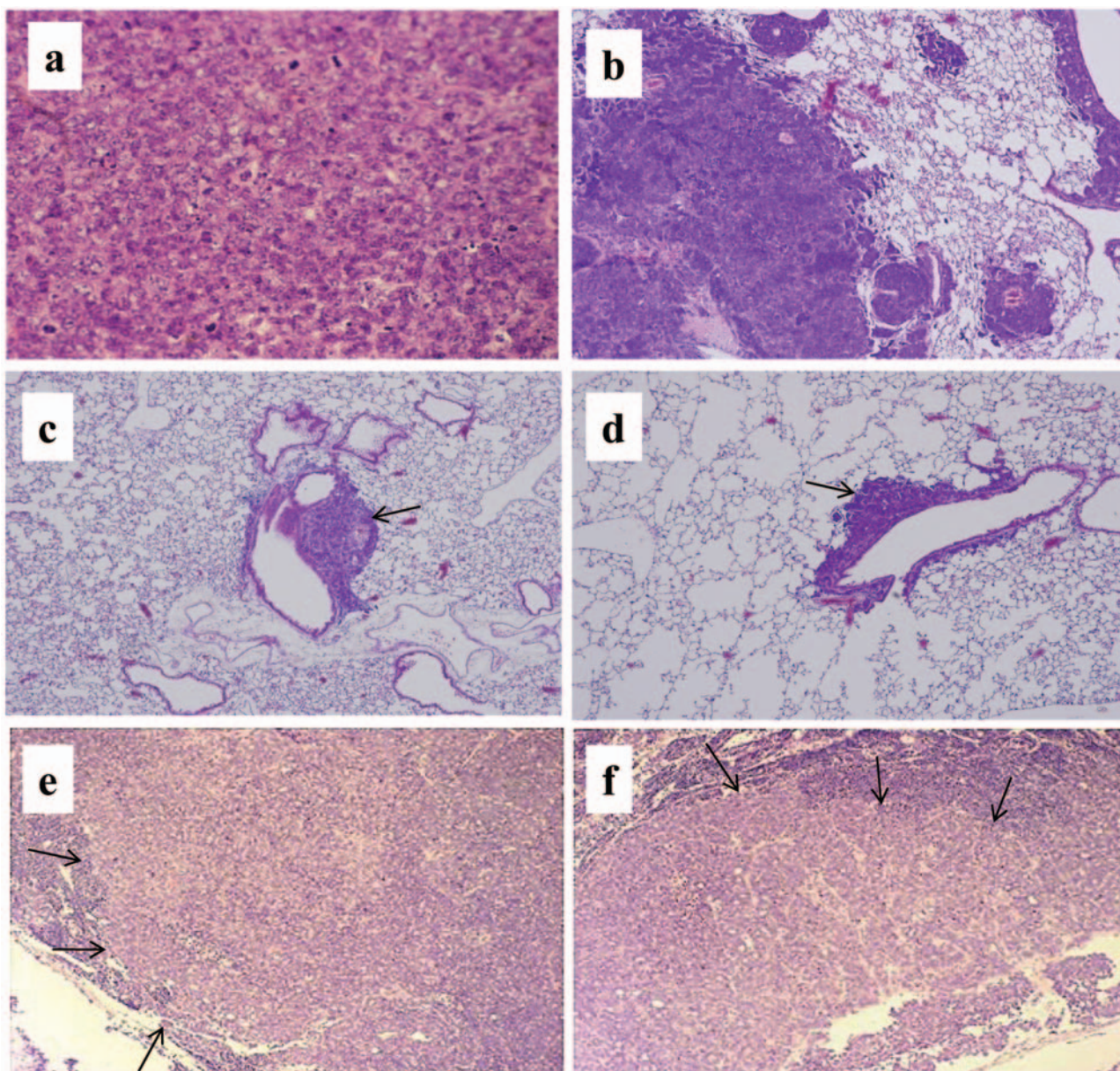


Figure 2. Histopathological analysis of mammary tumors in mice treated with panaxanthone. *a*, The implanted mammary tumors in a control mouse, $\times 400$. *b*, Metastatic foci in the lung of a control mouse. Many metastatic foci and nodules were seen in the control mice ($\times 40$). Metastatic foci (an arrow) in the lungs of mice given 2,500 (*c*) and 5,000 ppm (*d*) panaxanthone. Metastatic lung foci were much smaller in the treated groups than in the control group ($\times 40$). *e*, Metastasis to a lymph node occurred 57% of control mice, $\times 100$. Metastatic carcinoma cells (arrows) were filled with sinusoidal space ($\times 100$). *f*, Lymph node metastasis occurred in 29% of mice given 5,000 ppm panaxanthone. Metastatic tumor cells (arrows) were also observed in sinusoidal space ($\times 100$). (*a*)-(f), H&E stain.

sequential sections stained with hematoxylin and eosin (H&E) for histopathological examination and the remainder reserved unstained for immunohistochemistry.

Cell proliferation in mammary tumors. Immunohistochemistry was conducted using the avidin-biotin immunohistochemical complex method (LSAB kit; Dako Co., Carpinteria, CA, USA). Anti-PCNA mouse monoclonal Ab (PC-10; Dako Co.) was used at a dilution of

1:400. To evaluate cell kinetics, the number of PCNA-immunoreactive cells in late G₁- to S-phase, and G₂-phase per 1,000-5,000 cells was counted in the mammary glands and expressed as a percentage of all mammary tumor cells.

Apoptosis in mammary tumors. For quantitative analysis of apoptosis, sections from paraffin-embedded tumors were assayed using the terminal deoxynucleotidyl transferase-mediated dUTP-

FITC nick end-labeling (TUNEL) method using an apoptosis *in situ* detection kit (Wako Pure Chemical Industries, Osaka, Japan). TUNEL-positive cells were counted in viable regions peripheral to areas of necrosis in 5,000 cells within five randomly selected high power ($\times 200$) fields and the data expressed as percentages.

Microvessel densities in mammary tumors. To quantitatively assess blood microvessel density in the primary mammary carcinomas, immunohistochemistry was performed as described above. A rabbit polyclonal antibody against the von Willebrand factor (vWF; Dako Co.) was used. The number of immunopositive microvessels was counted as described elsewhere (16). Briefly, the slides were scanned at low-power ($\times 100$) magnification to identify those areas of highest microvascular density and these areas were then selected and counted at higher ($\times 200$ - 400) magnification to obtain mean \pm SD values.

In vitro study of the effects of α -mangostin on BJMC3879 cells. Cell viability: BJMC3879 cells were grown in RPMI-1640 medium supplemented with 10% (v/v) heat-inactivated fetal bovine serum and 2 mM L-glutamine under an atmosphere of 95% air and 5% CO₂ at 37°C. BJMC3879 cells were plated one day before α -mangostin treatment at 1×10^3 cells/well in 96-well plates. They were subsequently incubated for 24 h with culture medium containing vehicle (DMSO) alone or with medium containing α -mangostin at different concentrations up to 18 μ M. Cell viability was determined using a CellTiter-Blue Cell Viability Assay (Promega Co., Madison, WI, USA).

Cell-cycle distribution: BJMC3879 cells were grown in 2-well chamber slides (Lab-TekII; Nalgen Nunc International, Naperville, IL, USA), treated with 8 μ M α -mangostin for 24 h and fixed in cold 70% ethanol. Nuclear DNA was stained with a 50 μ g/ml propidium iodide solution containing 100 μ g/ml RNase A for 30 min at 37°C for cell cycle analysis. Cell cycle phases were determined with a microscope-based multiparameter laser scanning cytometer (LSC2; Olympus Optical Co., Tokyo, Japan) and the resulting data analyzed with WinCyt software (Compucyte Co., MA, USA).

TUNEL assay and caspase activity: BJMC3879 cells, grown in 2-well chamber slides and treated with 8 μ M α -mangostin for 24 h, were fixed in 4% formaldehyde solution in phosphate buffer and the TUNEL staining procedure performed as described for the *in vivo* study. The numbers of TUNEL-positive cells per 1,000 cells counted in four random high power ($\times 400$) fields by conventional light microscopy were expressed as a percentage of the total cells counted.

The activities of caspase-8, caspase-9 and caspase-3 were measured in cells treated with 8 μ M α -mangostin for 24 h using a fluorometric protease assay kit (MBL, Inc., Nagoya, Japan) in which cells were lysed with 0.1% Triton[®] X-100 lysis buffer and the protein concentration adjusted to 25 μ g in each sample. Caspase activity was measured in terms of fluorescence intensity using a VersaFluor fluorometer (Bio-Rad, Hercules, CA, USA).

Mitochondrial membrane potential ($\Delta\Psi$): Values for mitochondrial $\Delta\Psi$ in α -mangostin-treated and control cells were measured using a fluorescent cationic dye, 5,5',6,6'-tetrachloro-1,1',3,3'-tetraethyl-benzamidazolocarboxyanin iodide (JC-1) (Mitochondrial Membrane Potential Detection Kit; Cell Technology Inc, Mountain View, CA, USA) 3 h after α -mangostin treatment. Mitochondrial $\Delta\Psi$ was determined in terms of relative fluorescence units (RFU) using a VersaFluor fluorometer (Bio-Rad) with a 485 to 495 nm excitation filter and a 585 to 595 nm emission filter.

Caspase inhibitor experiment: For the caspase inhibitor experiments, 2 hours prior to 8 μ M α -mangostin exposure, the cells were treated with the caspase inhibitors as follows: 10 μ M and 100 μ M z-DEVD-fmk against caspase-3, z-IETD-fmk against caspase-8 and z-LEHD-fmk against caspase-9 for 48 h. Cell viability was measured using a fluorescent assay kit (CellTiter-Blue Cell Viability Assay; Promega) and then the activities of caspase-3, caspase-8 and caspase-9 were measured using a luminescent assay kit (Promega). The caspase activity data was then adjusted to account for the corresponding cell viability as previously reported (17).

Statistical analysis. Data for the dose-response effects were subjected to analysis of variance, while Tukey's test was employed for assessment of differences between means. Data from the cytometric studies, mitochondrial $\Delta\Psi$ analyses, caspase activity studies and caspase inhibition studies were compiled and compared between control and α -mangostin-treated groups using a two-sided Student's *t*-test.

Results

Food consumption and panaxanthone intake. The average food consumption was 6.0 g/day/mouse in the control group, 5.2 g/day/mouse in the 2,500 ppm group and 5.1 g/day/mouse in the 5,000 ppm group. The average panaxanthone intake was 543 mg/kg/day/mouse in the 2,500 ppm group and 1078 mg/kg/day/mouse in the 5,000 ppm group (Table I).

Body weights and general condition of mice. The body weights of control and panaxanthone-treated mice bearing mammary tumors did not differ statistically and are summarized in Figure 1a. A total of 2 mice (one mouse from each of the control and 5,000 ppm groups) died during weeks 3-4 as a result of carcinoma growth in the abdomen due to implantation failure. The general condition of all the other animals remained good throughout the study. The mice were terminated 8 weeks after the start of panaxanthone treatment, when the largest tumor in the control group was 2.0 cm in diameter.

Tumor growth. Tumor volumes are presented in Figure 1b. Significant reductions in tumor volume were evident in mice receiving 2,500 ppm panaxanthone from week 3, and in mice receiving 5,000 ppm panaxanthone from week 2. By the end of the experiment, the average tumor volume in the control animals was $1,749 \pm 469$ mm³, while that in the 2,500 and 5,000 ppm panaxanthone-treated groups was 939 ± 197 mm³ and 698 ± 243 mm³, respectively.

Lung and lymph node metastasis. Histopathologically, the mammary carcinomas induced by BJMC3879 cell inoculation proved to be moderately differentiated adenocarcinomas (Figure 2a). Lung metastasis occurred in 93% of controls, in 86% of the animals receiving 2,500 ppm panaxanthone and in 75% of the animals given

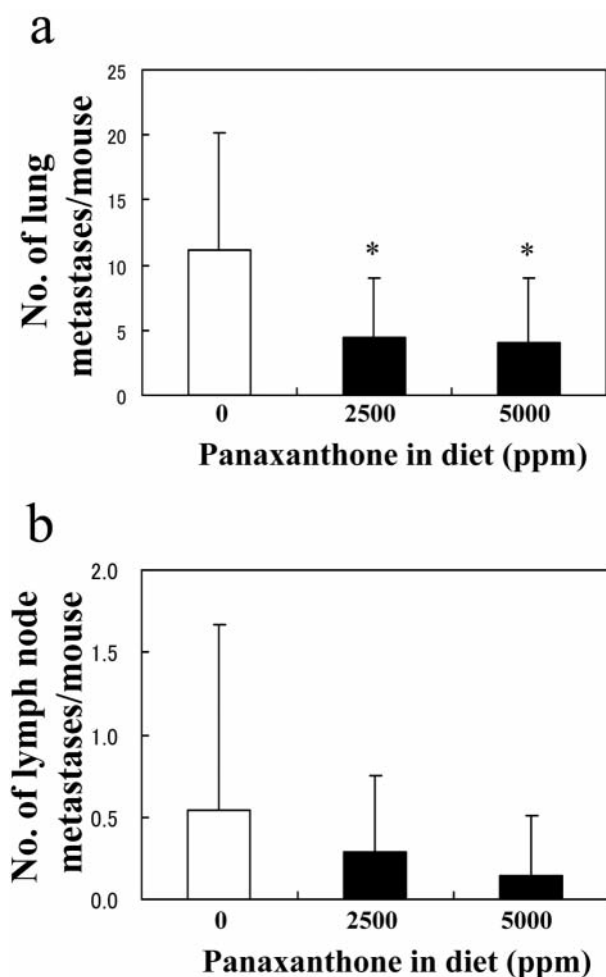


Figure 3. *a*, The multiplicity of lung metastasis was significantly lower in the 2,500 and 5,000 ppm panaxanthone-treated groups ($*p<0.05$). *b*, The multiplicity of lymph node metastasis was also lower in the panaxanthone-treated groups, but not significantly. Data represent mean \pm SD.

5,000 ppm panaxanthone, with no statistically significant variation. However, the metastatic foci tended to be markedly smaller in both panaxanthone-treated groups (Figure 2c, d) than in the control animals (Figure 2b). In the quantitative analysis, metastatic foci 250 μ m in diameter were counted, and significant decreases in the 2,500 and 5,000 ppm panaxanthone-treated groups were noted ($p<0.05$ compared with control) (Figure 3a). Lymph node metastasis occurred in 57% of controls (Figure 2e), in 36% of the animals receiving 2,500 ppm panaxanthone and in 29% of the animals given 5,000 ppm panaxanthone (Figure 2f). The number of metastasis-positive lymph nodes per mouse tended to decrease in a dose-dependent manner, but statistical significance was not attained because of large variations in control animals (Figure 3b).

Cell proliferation and apoptosis. Representative PCNA-positive cells (PCNA is regarded as a cell proliferation marker) from tumors from panaxanthone-treated and control animals are shown in Figure 4a and b. The number of PCNA-positive cells in tumors was significantly lower in the 2,500 and 5,000 ppm panaxanthone-treated groups compared to the control group ($p<0.01$) (Figure 5a). Representative TUNEL-positive cells from panaxanthone-treated and control animals are shown in Figure 4c and d. The number of TUNEL-positive cells in tumors was significantly greater in the 5,000 ppm panaxanthone-treated group compared to the control group ($p<0.05$) (Figure 5b).

Microvessel densities in mammary tumors. Representative tumor microvessels are illustrated in Figure 4e and f. A significant decrease in microvessel density was evident in the 2,500 and 5,000 ppm panaxanthone-treated groups compared to the control group (Figure 5c).

Cell viability, cell-cycle distribution and apoptosis in vitro. Inhibition of cell viability was seen in α -mangostin-treated cells in a dose-dependent manner, with statistical significance evidence from 8 μ M α -mangostin, compared with the control ($p<0.01$) (Figure 6a). Laser scanning cytometry of BJMC3879 cells stained with propidium iodide indicated that α -mangostin both increased the number of cells in G₁ arrest and suppressed the number entering the S- and G₂/M-phases (Figure 6b). Quantitative analysis revealed a significant increase in the number of TUNEL-positive cells after 24 h of 8 μ M α -mangostin treatment, compared with control cells ($p<0.01$) (Figure 6c).

Apoptosis signaling pathway. Significantly elevated activities of caspase-3 ($p<0.01$), caspase-9 ($p<0.01$), and caspase-8 ($p<0.01$) were observed in BJMC3879 cells treated with 8 μ M α -mangostin for 24 h (Figure 7a). The mitochondrial $\Delta\Psi$ was significantly reduced in α -mangostin-treated cells compared with control cells in a dose-dependent manner ($p<0.05$) (Figure 7b). To determine whether caspase activation is necessary to induce α -mangostin-induced apoptosis, BJMC3879 cells were treated with caspase inhibitors. Combination treatment with 8 μ M α -mangostin and 100 μ M z-DEDV-fmk (caspase-3 inhibitor) and z-LEHD (caspase-9 inhibitor) significantly increased cell viability compared with α -mangostin alone. z-IETD-fmk (caspase-8 inhibitor) slightly reduced cell death but not statistically significant. It was considered that caspase-8 did not particularly participate in α -mangostin-induced cell death (Figure 8). This strongly suggests that the engagement of the mitochondria-mediated apoptotic mitochondrial $\Delta\Psi$ decreased upon exposure to α -mangostin.

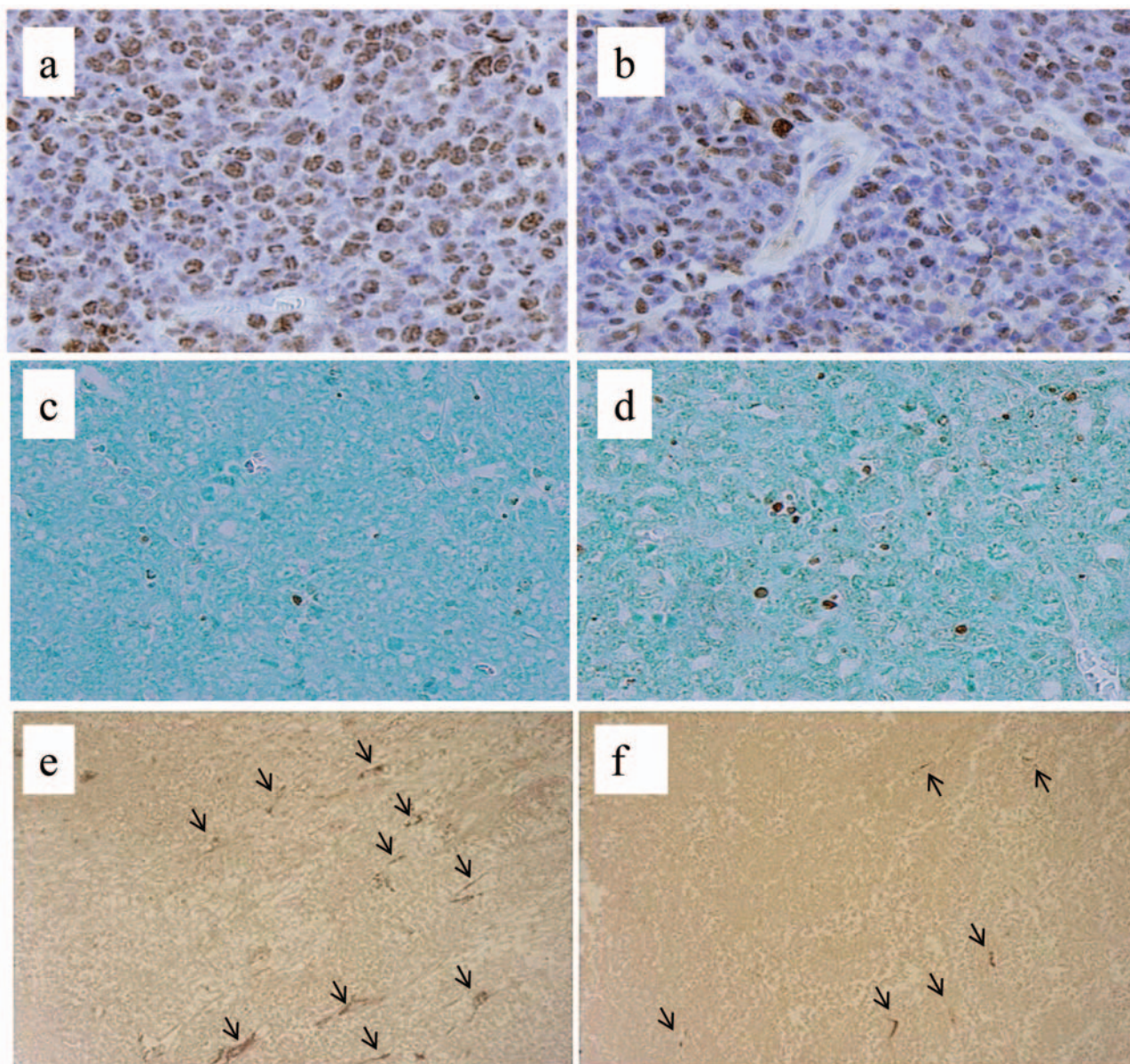


Figure 4. Many PCNA-positive cells were seen in the control group (a). The number of PCNA-positive cells tended to be lower in the 5,000 ppm group (b) than in the control group. $\times 400$. (a) and (b), PCNA immunohistochemistry. TUNEL-positive cells in mammary carcinomas in the panaxanthone-treated groups (d) much more frequent than in control mice (c); TUNEL, $\times 200$. Microvessel densities in mammary carcinomas were significantly greater in the 5,000 ppm panaxanthone-treated group (f) compared to the control group (e). Arrows indicate vWF-positive endothelial cells. $\times 200$. (e) and (f), vWF immunohistochemistry.

Discussion

In the present study, the antitumor activity of panaxanthone, which included suppression of tumor growth and a significant reduction in the number of lung metastases per mouse, was associated with elevation of apoptotic cell death, inhibition of PCNA and inhibition of microvessel density. Incidence and multiplicity of lymph node metastasis tended

to decrease in a dose-dependent manner but were not statistically significant because of large variations in control animals. In the *in vitro* studies, the effects of α -mangostin, which comprises approximately 80% of panaxanthone, on BJMC3879 cells included induction of apoptosis, inhibition of DNA synthesis and cell cycle arrest in the G_1 -phase.

Breast cancer is one of the leading causes of cancer mortality in women throughout the world, including Japan.

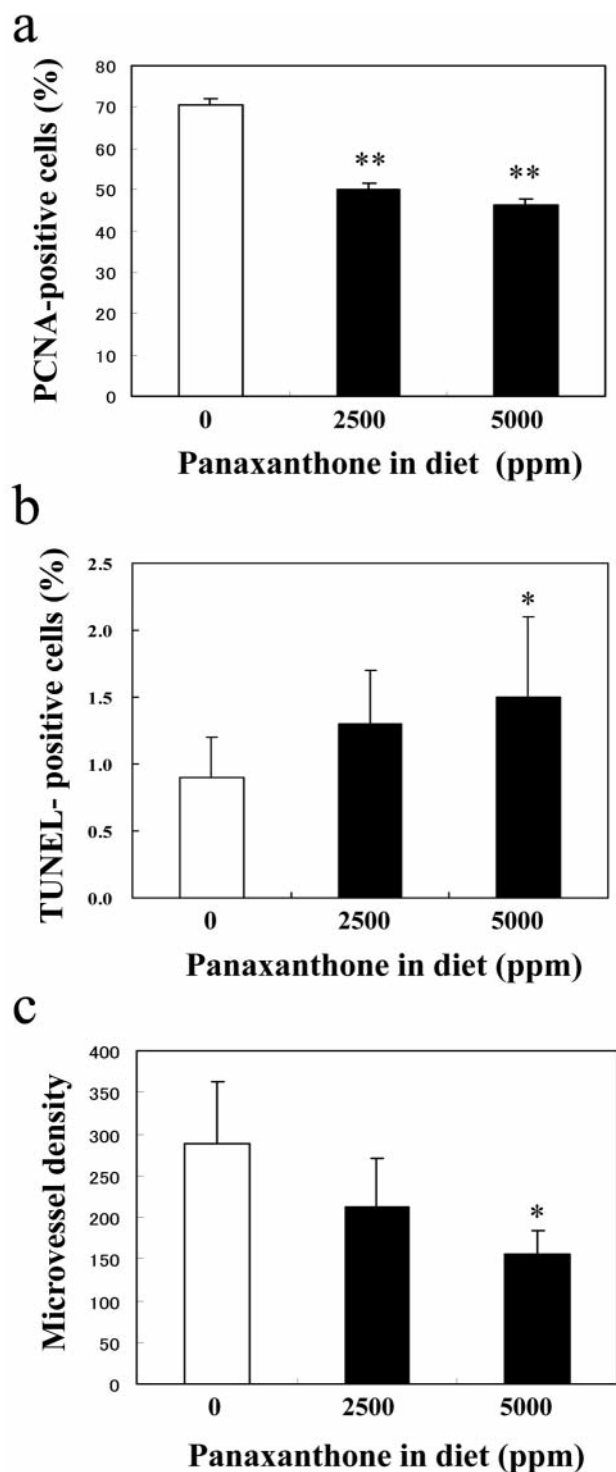


Figure 5. *a*, Cell proliferation in tumor cells, assessed by PCNA immunohistochemistry, was significantly lower in mice receiving 2,500 or 5,000 ppm panaxanthone-treated groups (** $p < 0.01$). *b*, The number of TUNEL-positive cells significantly increased in the 5,000 ppm panaxanthone-treated group as compared with tumors from control mice (* $p < 0.05$). Data represent mean \pm SD. *c*, Microvessel density in tumors, inferred by vWF-positive endothelium, was significantly lower in the 5,000 ppm panaxanthone-treated group (* $p < 0.05$).

The mean survival of breast cancer patients with metastasis to the lymph nodes, lung, liver, bone and brain is only 18 to 24 months, and responses to chemotherapy or endocrine therapy are limited to ~50% (18). Carter *et al.* reported that tumor size and nodal status are practical parameters for estimating disease prognosis. The lethal metastatic proclivity of mammary cancer explains the clinical importance of this disease. Patients presenting with metastatic disease are frequently incurable and reportedly, once breast carcinomas reach >4 cm, the chance of tumor recurrence or metastasis increases dramatically (19). Therefore, a treatment that offered suppression of metastasis, such as that involving xanthenes, would have significant clinical implications.

The xanthenes are known to induce apoptosis (5-9). The present study demonstrates that panaxanthone and α -mangostin significantly induce apoptosis in murine mammary carcinoma cells both *in vivo* and *in vitro*. There are two pathways currently thought to play a major role in the regulation of this type of mammalian cell death: an extrinsic pathway mediated by one or more death receptors involving caspase-8 and caspase-3, and an intrinsic pathway mediated by mitochondria involving caspase-9 and caspase-3 (20, 21). In the present study, we confirmed that panaxanthone-induced cell death involved apoptosis rather than necrosis, as determined using the TUNEL assay. We demonstrated in this experiment that panaxanthone induced increases in the activities of caspase-3, caspase-8, and caspase-9 and reduced the mitochondria-membrane potential in the BJMC3879 mammary carcinoma cells. Although elevated caspase-8, caspase-9 and caspase-3 activities were observed in our panaxanthone-treated cells, the fact that panaxanthone-treated cell death was reduced by inhibitors specific for caspase-9 and caspase-3 (z-LEHD-fmk and z-DEVD-fmk, respectively) strongly suggests that the intrinsic mitochondrial pathway is engaged in xanthone-induced apoptosis. However, cell death induced by α -mangostin was not statistically reduced by the addition of caspase-8 inhibitor (z-IETD-fmk) and thus this enzyme may not particularly participate in α -mangostin-induced apoptosis. Previous studies have found that lovastatin (14) and raloxifene (22) induce the same caspase activity pattern as the present study. Thus, caspase-8 may be downstream of both caspase-3 and caspase-9 (23).

Since 50% of human carcinomas have mutations in *p53* (24), as did the present cell line (14), the fact that a xanthone induced a *p53*-independent apoptotic response may be highly relevant to treating human neoplasms. In the present study, these xanthenes induced apoptosis in BJMC39879 cells that contained *p53* mutations. Our laser scanning cytometric analysis *in vitro* demonstrated that these xanthenes inhibited DNA synthesis and cell growth with arrest at G₁ and reduced transition to the S- and G₂/M-phases of the cell cycle, in line with a significant decrease in PCNA-positive cells. In fact, it has been shown that xanthenes increase expression of p27 and cdc2, which may be related to up-regulation of these cell cycle inhibitory proteins (9). It has

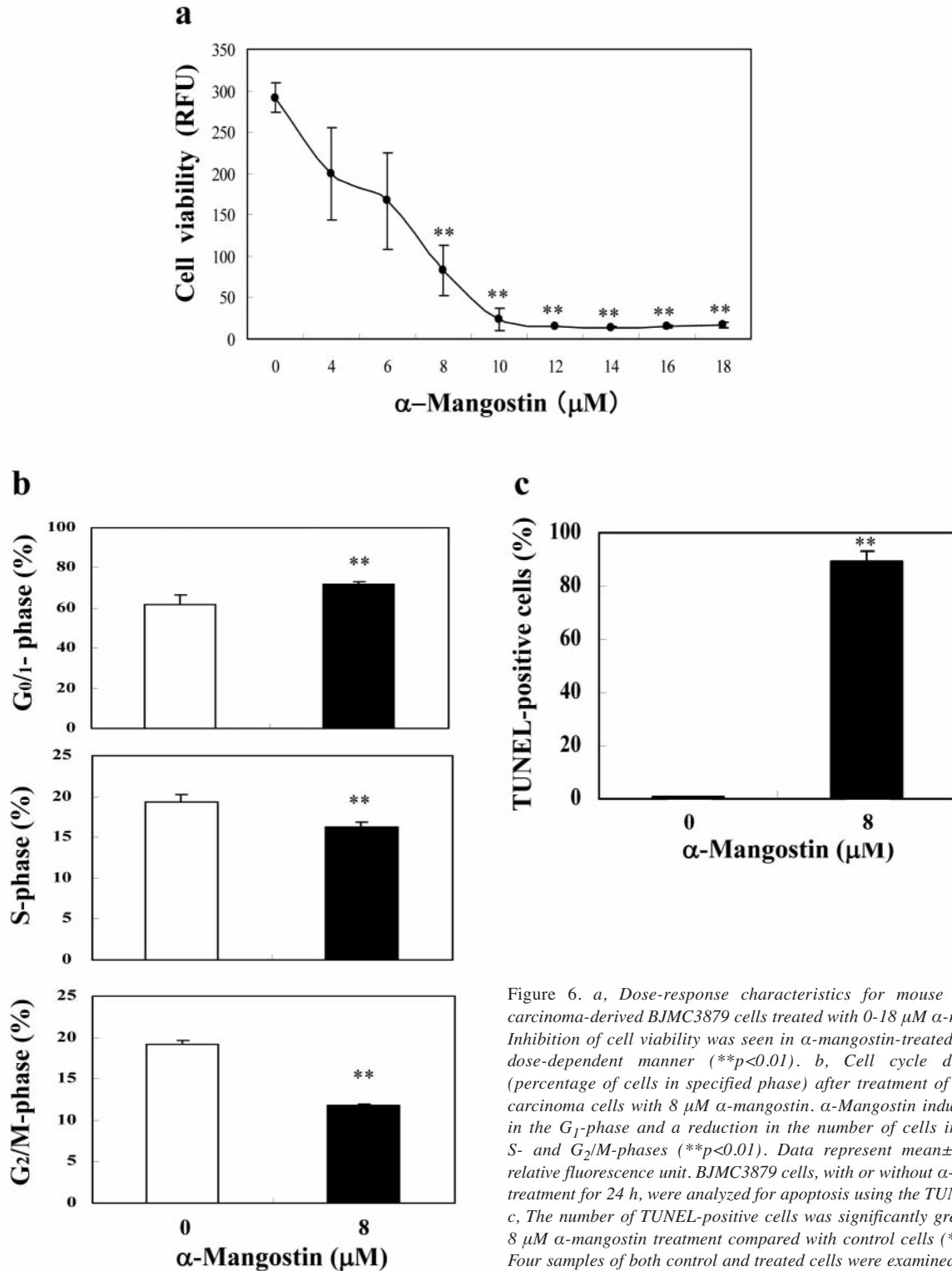


Figure 6. a, Dose-response characteristics for mouse mammary carcinoma-derived BJMC3879 cells treated with 0-18 μ M α -mangostin. Inhibition of cell viability was seen in α -mangostin-treated cells in a dose-dependent manner (** $p < 0.01$). b, Cell cycle distribution (percentage of cells in specified phase) after treatment of mammary carcinoma cells with 8 μ M α -mangostin. α -Mangostin induced arrest in the G₁-phase and a reduction in the number of cells in both the S- and G₂/M-phases (** $p < 0.01$). Data represent mean \pm SD. RFU, relative fluorescence unit. BJMC3879 cells, with or without α -mangostin treatment for 24 h, were analyzed for apoptosis using the TUNEL assay. c, The number of TUNEL-positive cells was significantly greater upon 8 μ M α -mangostin treatment compared with control cells (** $p < 0.01$). Four samples of both control and treated cells were examined.

also been reported that p27 overexpression induces apoptosis in several cell lines (25, 26), and cyclin and cdc2 suppression has been implicated in the apoptosis of cancer cells (27-30).

Angiogenesis, the process of new blood vessel formation, is considered critical for the growth of tumors and has been shown to correlate with poor prognosis in human colon cancer

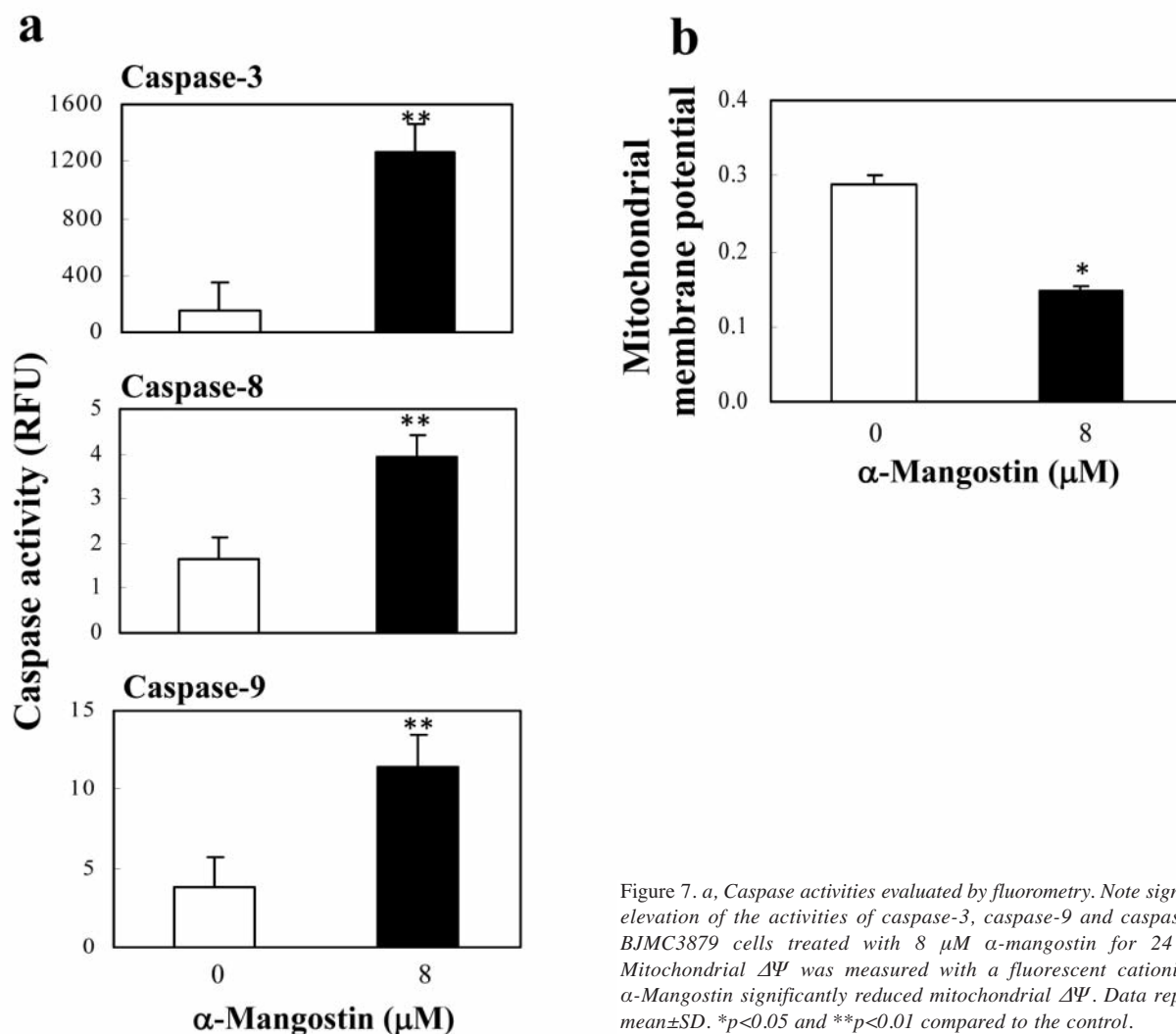


Figure 7. *a*, Caspase activities evaluated by fluorometry. Note significant elevation of the activities of caspase-3, caspase-9 and caspase-8 in BJMC3879 cells treated with 8 μ M α -mangostin for 24 h. *b*, Mitochondrial $\Delta\Psi$ was measured with a fluorescent cationic dye. α -Mangostin significantly reduced mitochondrial $\Delta\Psi$. Data represent mean \pm SD. * p <0.05 and ** p <0.01 compared to the control.

(31). In the present study, we demonstrated that the multiplicities of microvessel density and pulmonary metastasis were significantly lower in the panaxanthone-treated group. Neovascularization is a key process in the growth of solid tumors and the growth of both primary tumor and metastases is thus angiogenesis-dependent (32). It has been reported that γ -mangostin inhibits COX-2 expression (4). Pronounced COX-2 expression is clearly seen in colon cancer. (33). In fact, a COX-2 inhibitor, celecoxib, has been shown to reduce tumor growth and lung metastasis in our mammary cancer model (34).

In conclusion, a reduction in both the growth of the primary tumor and metastases was observed in the panaxanthone (α -mangostin 80%, γ -mangostin 20%)-treated groups. These antitumor effects, which involved induction of apoptosis, inhibition of DNA synthesis, cell cycle arrest in the G₁-phase and a reduction of angiogenesis, may be useful for chemoprevention and adjuvant therapy.

Acknowledgements

This study was partially supported by the High-Tech Research Center Grant at Osaka Medical College. We thank Dr. H. Tosa (Field & Device Co., Osaka, Japan), Mr. Y. Matoba (PM Rikken Yakka Co. Ltd., Nara, Japan) and Mr. H. Fujisawa (Sanko Medical Co. Ltd., Gifu, Japan) who supported our experiments.

References

- 1 Surh YJ: Cancer chemoprevention with dietary phytochemicals. *Nat Rev Cancer* 3: 768-780, 2003.
- 2 Huang YL, Chen CC, Chen YJ, Huang RL and Shieh BJ: Three xanthones and a benzophenone from *Garcinia mangostana*. *J Nat Prod* 64: 903-906, 2001.
- 3 Iinuma M, Tosa H, Tanaka T, Asai F, Kobayashi Y, Shimano R and Miyauchi K: Antibacterial activity of xanthones from guttiferaceous plants against methicillin-resistant *Staphylococcus aureus*. *J Pharm Pharmacol* 48: 861-865, 1996.

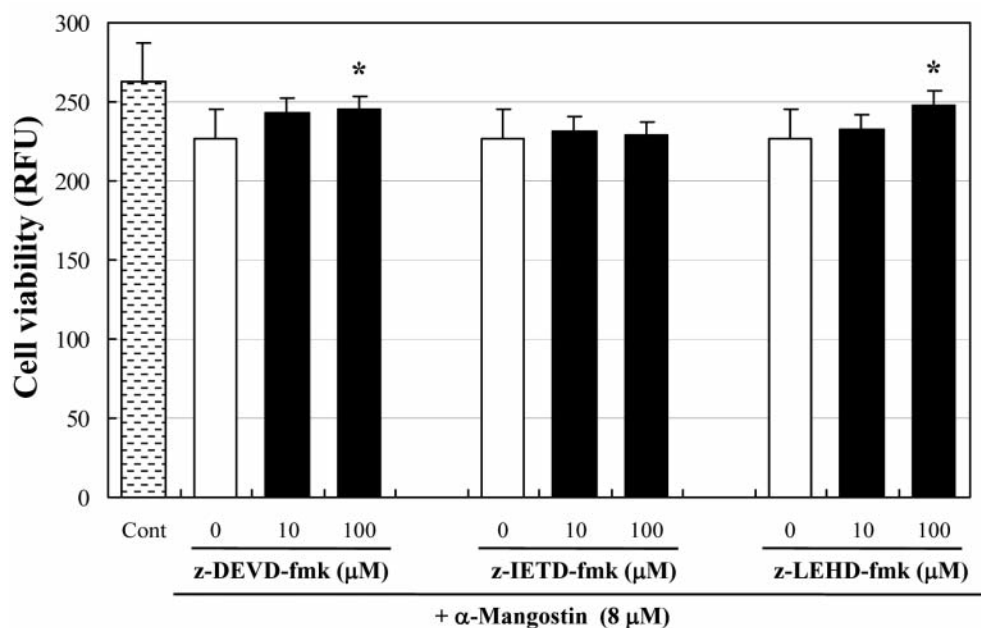


Figure 8. Cell viability was determined in mammary carcinoma cells treated with 8 μM α -mangostin with or without exposure to either 10 or 100 μM caspase inhibitors. Cell viability (%) was significantly increased by the caspase-3 inhibitor zDEVD-fmk (* $p < 0.05$) and by the caspase-9 inhibitor z-LEHD-fmk (* $p < 0.05$) at the 100 μM concentration only. However, cell viability was unaffected by addition of any concentration of the caspase-8 inhibitor z-IETD-fmk. Data represent mean \pm SD. RFU, relative fluorescence unit.

- 4 Nakatani K, Yamakuni T, Kondo N, Arakawa T, Oosawa K, Shimura S, Inoue H and Ohizumi Y: γ -Mangostin inhibits inhibitor-kappaB kinase activity and decreases lipopoly-saccharide-induced cyclooxygenase-2 gene expression in C6 rat glioma cells. *Mol Pharmacol* 66: 667-674, 2004.
- 5 Matsumoto K, Akao Y, Kobayashi E, Ohguchi K, Ito T, Tanaka T, Iinuma M and Nozawa Y: Induction of apoptosis by xanthenes from mangosteen in human leukemia cell lines. *J Nat Prod* 66: 1124-1127, 2003.
- 6 Matsumoto K, Akao Y, Yi H, Ohguchi K, Ito T, Tanaka T, Kobayashi E, Iinuma M and Nozawa Y: Preferential target is mitochondria in alpha-mangostin-induced apoptosis in human leukemia HL60 cells. *Bioorg Med Chem* 12: 5799-5806, 2004.
- 7 Sato A, Fujiwara H, Oku H, Ishiguro K and Ohizumi Y: Alpha-mangostin induces Ca^{2+} -ATPase-dependent apoptosis via mitochondrial pathway in PC12 cells. *J Pharmacol Sci* 95: 33-40, 2004.
- 8 Moongkarndi P, Kosem N, Kaslungka S, Luanratana O, Pongpan N and Neungton N: Antiproliferation, antioxidation and induction of apoptosis by *Garcinia mangostana* (mangosteen) on SKBR3 human breast cancer cell line. *J Ethnopharmacol* 90: 161-166, 2004.
- 9 Matsumoto K, Akao Y, Ohguchi K, Ito T, Tanaka T, Iinuma M and Nozawa Y: Xanthenes induce cell-cycle arrest and apoptosis in human colon cancer DLD-1 cells. *Bioorg Med Chem* 13: 6064-6069, 2005.
- 10 Beslija S, Bonnetterre J, Burstein H, Cocquyt V, Gnatt M, Goodwin P, Heinemann V, Jassem J, Kostler WJ, Krainer M, Menard S, Petit T, Petruzella L, Possinger K, Schmid P, Stadtmauer E, Stockler M, Van Belle S, Vogel C, Wilcken N, Wiltshcke C, Zielinski CC and Zwierzina H: Second consensus on medical treatment of metastatic breast cancer. *Ann Oncol* 18: 215-225, 2007.
- 11 Japan Research Group for Publication-based Cancer Regulation in Japan: Estimates based on data from 12 population-based cancer registries. *Jpn J Clin Oncol* 33: 241-245, 2003.
- 12 Hortobagyi GN: Can we cure limited metastatic breast cancer? *J Clin Oncol* 20: 620-623, 2002.
- 13 Shibata MA, Morimoto J and Otsuki Y: Suppression of murine mammary carcinoma growth and metastasis by HSVtk/GCV gene therapy using *in vivo* electroporation. *Cancer Gene Ther* 9: 16-27, 2002.
- 14 Shibata MA, Ito Y, Morimoto J and Otsuki Y: Lovastatin inhibits tumor growth and lung metastasis in mouse mammary carcinoma model: a p53-independent mitochondrial-mediated apoptotic mechanism. *Carcinogenesis* 25: 1887-1898, 2004.
- 15 Shibata MA, Liu M-L, Knudson MC, Shibata E, Yoshidome K, Bandy T, Korsmeyer SJ and Green JE: Haploid loss of *bax* leads to accelerated mammary tumor development in C3(1)/SV40-TAg transgenic mice: reduction in protective apoptotic response at the preneoplastic stage. *EMBO J* 18: 2692-2701, 1999.
- 16 Gorrin-Rivas MJ, Arii S, Furutani M, Mizumoto M, Mori A, Hanaki K, Maeda M, Furuyama H, Kondo Y and Imamura M: Mouse macrophage metalloelastase gene transfer into a murine melanoma suppresses primary tumor growth by halting angiogenesis. *Clin Cancer Res* 6: 1647-1654, 2000.
- 17 Shibata MA, Akao Y, Shibata E, Nozawa Y, Ito T, Mishima S, Morimoto J and Otsuki Y: Vatanol C, a novel resveratrol tetramer, reduces lymph node and lung metastases of mouse mammary carcinoma carrying p53 mutation. *Cancer Chemother Pharmacol* 60: 681-691, 2007.

- 18 Ellis M, Hayes D and Lippman M: Treatment of metastatic breast cancer. *In*: Disease of the Breast. Harris JR, Lippman ME, Morrow M and Osborne CK (eds.). Lippincott Williams & Wilkins, Philadelphia, PA, USA pp. 794-797, 2000.
- 19 Carter CL, Allen C and Henson DE: Relation of tumor size, lymph node status, and survival in 24,740 breast cancer cases. *Cancer* 63: 181-187, 1989.
- 20 Hengartner MO: The biochemistry of apoptosis. *Nature* 407: 770-776, 2000.
- 21 Otsuki Y: Tissue specificity of apoptotic signal transduction. *Med Electron Microsc* 37: 163-169, 2004.
- 22 Morishima S, Shibata MA, Ohmichi M and Otsuki Y: Raloxifene, a selective estrogen receptor modulator, induces mitochondria-mediated apoptosis in human endometrial carcinoma cells. *Med Mol Morphol* 41: 132-138, 2008.
- 23 Cha YJ, Kim HS, Rhim H, Kim BE, Jeong SW and Kim IK: Activation of caspase-8 in 3-deazaadenosine-induced apoptosis of U-937 cells occurs downstream of caspase-3 and caspase-9 without Fas receptor-ligand interaction. *Exp Mol Med* 33: 284-292, 2001.
- 24 Greenblatt MS, Bennett WP, Hollstein M and Harris CC: Mutations in the *p53* tumor suppressor gene: clues to cancer etiology and molecular pathogenesis. *Cancer Res* 54: 4855-4878, 1994.
- 25 Wang X, Gorospe M, Huang Y and Holbrook NJ: p27^{Kip1} overexpression causes apoptotic death of mammalian cells. *Oncogene* 15: 2991-2997, 1997.
- 26 Katayose Y, Kim M, Rakkar AN, Li Z, Cowan KH and Seth P: Promoting apoptosis: a novel activity associated with the cyclin-dependent kinase inhibitor p27. *Cancer Res* 57: 5441-5445, 1997.
- 27 Yuan J, Yan R, Kramer A, Eckerdt F, Roller M, Kaufmann M and Strebhardt K: Cyclin B1 depletion inhibits proliferation and induces apoptosis in human tumor cells. *Oncogene* 23: 5843-5852, 2004.
- 28 Kamasani U, Huang M, Duhadaway JB, Prochownik EV, Donover PS and Prendergast GC: Cyclin B1 is a critical target of RhoB in the cell suicide program triggered by farnesyl transferase inhibition. *Cancer Res* 64: 8389-8396, 2004.
- 29 Lai D, Weng S, Wang C, Qi L, Yu C, Fu L and Chen W: Small antisense RNA to cyclin D1 generated by pre-tRNA splicing inhibits growth of human hepatoma cells. *FEBS Lett* 576: 481-486, 2004.
- 30 O'Connor DS, Wall NR, Porter AC and Altieri DC: A p34(cdc2) survival checkpoint in cancer. *Cancer Cell* 2: 43-54, 2002.
- 31 Takahashi Y, Kitadai Y, Bucana CD, Cleary KR and Ellis LM: Expression of vascular endothelial growth factor and its receptor, KDR, correlates with vascularity, metastasis, and proliferation of human colon cancer. *Cancer Res* 55: 3964-3968, 1995.
- 32 Folkman J: Angiogenesis-dependent diseases. *Semin Oncol* 28: 536-542, 2001.
- 33 Eberhart CE, Coffey RJ, Radhika A, Giardiello FM, Ferrenbach S and DuBois RN: Up-regulation of *cyclooxygenase 2* gene expression in human colorectal adenomas and adenocarcinomas. *Gastroenterology* 107: 1183-1188, 1994.
- 34 Yoshinaka R, Shibata MA, Morimoto J, Tanigawa N and Otsuki Y: COX-2 inhibitor celecoxib suppresses tumor growth and lung metastasis of a murine mammary cancer. *Anticancer Res* 26: 4245-4254, 2006.

Received February 2, 2009

Revised May 6, 2009

Accepted May 12, 2009